Research paper

Struct Multidisc Optim 27, 435–445 (2004)
DOI 10.1007/s00158-004-0388-x

# Optimal shapes of parametrically excited beams

**A.A. Mailybaev, H. Yabuno, and H. Kaneko**

**Abstract** Straight elastically supported beams of variable width under the action of a periodic axial force are considered. Two shape optimization problems for reducing parametric resonance zones are studied. In the first problem, the minimal (critical) amplitude of the excitation force is maximized. In the second problem, the range of resonant frequencies is minimized for a given parametric resonance zone and a fixed amplitude of excitation. These two optimization problems are proved to be equivalent in the case of small external damping and small excitation force amplitude. It is shown that optimal designs have strong universal character, i.e. they depend only on the natural modes involved in the parametric resonance and boundary conditions. An efficient numerical method of optimization is developed. Optimal beam shapes are found for different boundary conditions and resonant modes. Experiments for uniform and optimal simply supported elastic beams have been conducted demonstrating a very good agreement with theoretical prediction.

**Key words** elastic beam, shape optimization, parametric resonance, singularity, sensitivity analysis, experiment

## 1 Introduction

Shape optimization of beams under stability criteria is an interesting and important topic from both the theoretical and practical point of view. On one hand, this problem requires sophisticated analytical and numerical methods for sensitivity analysis and knowledge on bifurcation and singularity theories. On the other hand, the correct formulation of the problem, including minimal width constraints and analysis of nonlinear behaviour, may strongly influence the practical use of optimal designs. We refer the reader to the surveys on optimal beam problems by Seyranian and Privalova (2003) for the case of static loads and by Langthjem and Sugiyama (2000) for the case of follower loads. Pedersen (1982–83) optimized beams under several natural frequency constraints. The optimal shape of a pipe conveying fluid was investigated by Langthjem (1996). Optimal shapes of a beam, minimizing the critical excitation amplitudes of primary parametric resonance zones, were analysed numerically by Seyranian *et al.* (2000). Very few experimental works on optimal beams are available in the literature (Langthjem 1996).

In this paper, we consider beams of rectangular cross-section with constant thickness and variable width. The length and total volume of the beam are fixed. Elastic supports at both ends are considered, which, in particular, include the cases of simply supported and clamped boundary conditions. Parametric resonance of the beam under a periodic axial force is studied. Two optimization problems are considered. In the first problem, the minimal (critical) amplitude of the excitation force is maximized. In the second problem, the range of resonant excitation frequencies is minimized for a given parametric resonance zone and a fixed amplitude of excitation. We prove that these two optimization problems are equivalent in the case of small external damping and a small excitation force amplitude. Moreover, we show that the optimal designs do not depend on the damping coefficient, on the value of the excitation amplitude in the second problem, or on the resonance number. All these properties reveal strong universal character of optimal beam shapes, which depend only on the natural modes involved in parametric resonance and on the boundary conditions. This universality is of great importance for practical use of optimal designs. Numerical computations show that the optimal shape changes weakly if the parametric excitation is applied to a prestressed beam

*Received: 19 January 2004*
*Published online: 4 May 2004*


A.A. Mailybaev[1,✉], H. Yabuno[2], and H. Kaneko[2]

[1] Institute of Mechanics, Moscow State Lomonosov University, Michurinsky pr. 1, 119192 Moscow, Russia
e-mail: mailybaev@imec.msu.ru
[2] Institute of Engineering Mechanics and Systems, University of Tsukuba, Tsukuba City 305-8573, Japan
e-mail: yabuno@aosuna.esys.tsukuba.ac.jp, kaneko@aosuna.esys.tsukuba.ac.jp

(with a static axial force lower than the critical Euler force).

In the analysis, we use explicit formulae obtained recently by Mailybaev and Seyranian (2001) (see also Seyranian and Mailybaev 2003), which describe the parametric resonance zones as half-cones in the three-parameter space (frequency and amplitude of parametric excitation and damping coefficient). As a result, the optimization problem is reduced to the minimization of an objective functional depending only on natural frequencies and modes involved in parametric resonance. This approach allows avoiding time-consuming multiple integrations of equations of motion required for stability analysis in the Floquet theory (e.g. Seyranian and Mailybaev 2003). Optimal beam shapes are found numerically for different boundary conditions and resonant modes.

Experiments on simple parametric resonance of the first mode are conducted for the uniform and optimal simply supported beams. The reduction of the resonance zone for the optimal beam is shown to be in very good agreement with theoretical prediction. Nonlinear response of the uniform and optimal beams is analysed experimentally.

Compared to the previous work by Seyranian *et al.* (2000), where the beam of circular cross-section was optimized, the present study has the following advantages. First, we use a more realistic model of external damping taking into account the beam width variation. We consider two different optimization problems and prove universality properties of our optimal designs. Finally, the gain in optimization attained in our study is about 17–22% (depending on the boundary conditions and width constraints), which is higher than the 4–9% obtained by Seyranian *et al.* (2000).

The paper is organized as follows. In Sect. 2, we describe the analytical model and basic equations. In Sect. 3, general formulae for parametric resonance zones are given. In Sect. 4, we formulate optimization problems, derive the objective functional, and prove the universality property of optimal designs. Section 5 describes the numerical optimization method. In Sect. 6, optimal solutions are found for different boundary conditions and resonant modes. Section 7 describes the experimental results. Finally, the conclusion summarizes the contribution and discusses the perspective for further investigation.

## 2
## Analytical model and basic equations

Let us consider a straight elastic beam of rectangular cross-section having a length $l$, a thickness $h$, and a variable width $s(x)$, see Fig. 1. The beam is loaded by a periodic axial force $p(t) = p_0 + \delta\varphi(\Omega t)$, where $\delta$ and $\Omega$ are the amplitude and frequency of parametric excitation, respectively, and $\varphi(t)$ is a periodic function of period $2\pi$. We study small vibrations of the beam in the $xy$-plane,

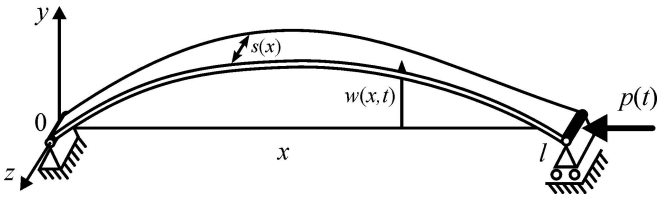


**Fig. 1** Beam of variable width under parametric excitation

see Fig. 1. A deflection of the beam at the position $x$ and time $t$ is denoted by $w(x,t)$. It is assumed that the beam is externally damped, and the damping force at the position $x$ is proportional to the velocity and width of the beam with the external damping coefficient $\gamma$. Then the equation of motion of the beam takes the form

$$\frac{\partial^2}{\partial x^2}\left(EI(x)\frac{\partial^2 w}{\partial x^2}\right) + p(t)\frac{\partial^2 w}{\partial x^2} + \gamma s(x)\frac{\partial w}{\partial t} + m(x)\frac{\partial^2 w}{\partial t^2} = 0\,, \tag{1}$$

where $E$ is the Young's modulus, $I(x)$ is the cross-sectional moment of inertia, and $m(x)$ is the mass of the beam per unit length. For beams of rectangular cross-section considered in this paper, we have $m(x) = \rho h s(x)$ and $I(x) = h^3 s(x)/12$, where $\rho$ is the density of the beam. The total volume of the beam, which is assumed to be fixed, equals

$$V_0 = h\int_0^l s(x)\,\mathrm{d}x = const\,. \tag{2}$$

Hence, the mass of the beam is fixed and equal to $\rho V_0$.

The external damping term $\gamma s(x)\partial w/\partial t$ in (1) takes into account the variation of the damping force due to the change of beam width. The damping coefficient $\gamma$ depends on the viscosity and density of the external media (gas or fluid) and on the frequency of beam vibrations (e.g. Batchelor 1999). Within a fixed parametric resonance zone, a change of the frequency of beam vibrations is small. Thus, the damping coefficient $\gamma$ can be assumed to be constant for each particular resonance number (zone).

As the boundary conditions, we consider the case of a beam elastically supported at both ends:

$$w(0,t) = w(l,t) = 0\,,$$
$$\left(-c_1\frac{\partial w}{\partial x} + EI\frac{\partial^2 w}{\partial x^2}\right)_{x=0} = \left(c_2\frac{\partial w}{\partial x} + EI\frac{\partial^2 w}{\partial x^2}\right)_{x=l} = 0\,, \tag{3}$$

where $c_1 \geq 0$ and $c_2 \geq 0$ are the elastic coefficients of the supports. The limit cases $c_1 = c_2 = 0$ and $c_1 = c_2 = \infty$ correspond to simply supported and clamped-clamped beams, respectively.

Let us consider free vibrations of the beam without periodic excitation ($\delta = 0$) and with no damping ($\gamma = 0$),

and assume that $p_0 < p_{\rm cr}$, i.e. the constant compressive force $p_0$ is lower than the static critical force of the beam $p_{\rm cr}$. Looking for a solution of (1) in the form $w(x,t) = u(x)\exp(i\omega t)$, we obtain the equation

$$\frac{\mathrm{d}^2}{\mathrm{d}x^2}\left(EI(x)\frac{\mathrm{d}^2u}{\mathrm{d}x^2}\right) + p_0\frac{\mathrm{d}^2u}{\mathrm{d}x^2} = \omega^2 m(x)u\,, \tag{4}$$

determining the eigenfrequencies $\omega$ and corresponding eigenmodes $u(x)$ of the beam prestressed by a constant force $p_0$. The boundary conditions for $u(x)$ are

$$u(0) = u(l) = 0\,,$$

$$\left(-c_1\frac{\mathrm{d}u}{\mathrm{d}x} + EI\frac{\mathrm{d}^2u}{\mathrm{d}x^2}\right)_{x=0} = \left(c_2\frac{\mathrm{d}u}{\mathrm{d}x} + EI\frac{\mathrm{d}^2u}{\mathrm{d}x^2}\right)_{x=l} = 0\,. \tag{5}$$

Let us introduce the following dimensionless variables and parameters:

$$t^* = \frac{h}{l^2}\sqrt{\frac{E}{12\rho}}\,t\,,\quad x^* = \frac{x}{l}\,,\quad w^* = \frac{w}{l}\,,\quad s^* = \frac{hl}{V_0}\,s\,,$$

$$p_0^* = \frac{12l^3}{h^2EV_0}\,p_0\,,\quad \delta^* = \frac{12l^3}{h^2EV_0}\,\delta\,,\quad \Omega^* = \frac{l^2}{h}\sqrt{\frac{12\rho}{E}}\,\Omega\,,$$

$$p^*(t^*) = p_0^* + \delta^*\varphi(\Omega^* t^*)\,,\quad \omega^* = \frac{l^2}{h}\sqrt{\frac{12\rho}{E}}\,\omega\,,$$

$$\gamma^* = \frac{l^2}{h^2}\sqrt{\frac{12}{E\rho}}\,\gamma\,,\quad c_1^* = \frac{12l^2}{h^2EV_0}\,c_1\,,\quad c_2^* = \frac{12l^2}{h^2EV_0}\,c_2\,\cdot \tag{6}$$

Then (1) is written in the dimensionless form as

$$(s(x)w'')'' + p(t)w'' + \gamma s(x)\dot{w} + s(x)\ddot{w} = 0 \tag{7}$$

with the boundary conditions

$$w(0,t) = w(1,t) = 0\,,$$

$$(-c_1w' + sw'')_{x=0} = (c_2w' + sw'')_{x=1} = 0\,, \tag{8}$$

where the dot ($\dot{}$) and prime ($'$) represent the derivatives with respect to $t^*$ and $x^*$, respectively. In (7), (8) and hereafter, the asterisk ($^*$) is omitted. The constant volume condition (2) becomes

$$\int_0^1 s(x)\,\mathrm{d}x = 1\,. \tag{9}$$

Finally, the equation for eigenmodes and eigenfrequencies (4) takes the form

$$(s(x)u'')'' + p_0u'' = \omega^2 s(x)u \tag{10}$$

with the boundary conditions

$$u(0) = u(1) = 0\,,$$

$$(-c_1u' + su'')_{x=0} = (c_2u' + su'')_{x=1} = 0\,. \tag{11}$$

## 3 Parametric resonance zones

Let $0 < \omega_1 < \omega_2 < \cdots$ be eigenfrequencies of free vibrations of the beam without parametric excitation and damping (all the eigenfrequencies are assumed to be distinct). The corresponding eigenmodes $u_1(x), u_2(x), \ldots$ determined by (10) with boundary conditions (11) can be chosen satisfying the normalization conditions

$$\int_0^1 su_i^2\,\mathrm{d}x = 1\,,\quad i = 1,2,\ldots\,. \tag{12}$$

If small parametric excitation is applied, the trivial equilibrium of the beam, $w(x,t) \equiv 0$, may become unstable (the parametric resonance occurs). For beams of variable cross-section, the parametric resonance may happen only if the excitation frequency $\Omega$ is close to the resonant value

$$\Omega_0 = \frac{\omega_i + \omega_j}{k}\,, \tag{13}$$

for some eigenfrequencies $\omega_i$, $\omega_j$ and a positive integer $k$ (e.g. Mailybaev and Seyranian 2001). The cases $i = j$ and $i \neq j$ are called simple and summed combination resonances, respectively. Difference combination resonances, corresponding to the excitation frequencies $\Omega_0 = (\omega_i - \omega_j)/k$, $i > j$, do not occur. For small excitation amplitudes $\delta$ and damping coefficients $\gamma$, we find the parametric resonance zones for system (7), (8) using the results of Mailybaev and Seyranian (2001) (see also Seyranian and Mailybaev 2003, Chap. 11) as follows

$$\gamma^2 - \frac{b_{ij}^2\left(a_k^2 + b_k^2\right)}{4\omega_i\omega_j}\,\delta^2 +$$

$$k^2\left(\Delta\Omega - \frac{c_0(\omega_i b_{jj} + \omega_j b_{ii})}{2k\omega_i\omega_j}\,\delta\right)^2 \le 0\,. \tag{14}$$

In this inequality,

$$\Delta\Omega = \Omega - \Omega_0\,,\quad b_{ij} = -\int_0^1 u_i'u_j'\,\mathrm{d}x\,, \tag{15}$$

and the quantities $a_k$, $b_k$, and $c_0$ are the Fourier coefficients and the mean value of the $2\pi$-periodic function $\varphi(t)$:

$$a_k = \frac{1}{\pi}\int_0^{2\pi}\varphi(t)\cos(kt)\,\mathrm{d}t\,,$$

$$b_k = \frac{1}{\pi}\int_0^{2\pi}\varphi(t)\sin(kt)\,\mathrm{d}t\,,\quad c_0 = \frac{1}{2\pi}\int_0^{2\pi}\varphi(t)\,\mathrm{d}t\,. \tag{16}$$

Inequality (14) defines a half-cone in the space of three parameters $(\Omega, \delta, \gamma)$, where $\gamma > 0$ is the physical restriction, see Fig. 2(a). The interior of the half-cone represents

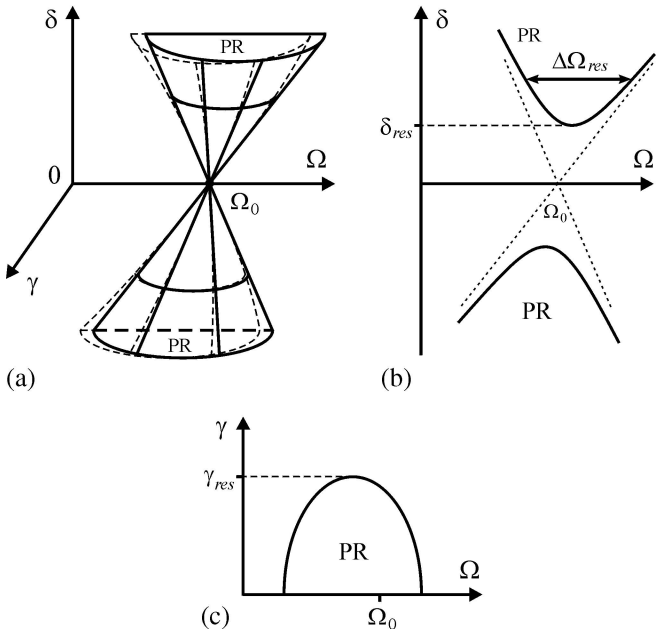


**Fig. 2** Parametric resonance zone (PR): (a) in $(\Omega, \delta, \gamma)$-space; first-order approximation (solid lines) and exact boundary (dashed lines), (b) in $(\Omega, \delta)$-plane for a fixed damping coefficient $\gamma$, (c) in $(\Omega, \gamma)$-plane for a fixed excitation amplitude $\delta$

the instability region corresponding to a given resonance number $k$. The cone surface is the first-order approximation of the stability boundary; it has a second-order deviation from the exact stability boundary at large values of $\delta$ and $\gamma$, see Fig. 2(a). The axis of the cone is vertical (parallel to the $\delta$-axis) if $c_0 = 0$, i.e. if the excitation function $\varphi(t)$ has zero mean value.

If the function $\varphi(t)$ is given by a finite Fourier series (e.g. $\varphi(t) = \cos t$), we have $a_k = b_k = 0$ for large resonance numbers $k$. If $a_k = b_k = 0$, the cone (14) degenerates into a single line. This means that the resonance zone either does not exist, or it is a sharp wedge with a single tangent at the point $(\Omega, \delta, \gamma) = (\Omega_0, 0, 0)$. As a classical example, in the Mathieu equation, all resonant zones starting with $k = 2$ are degenerate. In this paper, we consider resonances for which $a_k^2 + b_k^2 \neq 0$.

If the damping coefficient $\gamma > 0$ is fixed, a boundary of the parametric resonance zone is represented by hyperbolae in the $(\Omega, \delta)$-plane, see Fig. 2(b). The minimal absolute (critical) value of the excitation amplitude $\delta$, at which the parametric resonance may occur, is (see Mailybaev and Seyranian 2001)

$$\delta_{\rm res}(\gamma) = 2\gamma \sqrt{\frac{\omega_i \omega_j}{b_{ij}^2 (a_k^2 + b_k^2)}} \,. \tag{17}$$

If $\delta > \delta_{\rm res}$, the instability occurs for excitation frequencies belonging to a certain interval. The width of this resonant interval equals

$$\Delta\Omega_{\rm res}(\delta, \gamma) = \frac{1}{k} \sqrt{\frac{b_{ij}^2 \, (a_k^2 + b_k^2)}{\omega_i \omega_j} \, \delta^2 - 4\gamma^2} \,. \tag{18}$$

Using formulae obtained by Mailybaev and Seyranian (2001), we find the parametric resonance zones for the system without damping ($\gamma = 0$) as

$$\frac{b_{ij}^2 \, (a_k^2 + b_k^2)}{4\omega_i \omega_j} \, \delta^2 \geq k^2 \left( \Delta\Omega - \frac{c_0(\omega_i b_{jj} + \omega_j b_{ii})}{2k\omega_i \omega_j} \, \delta \right)^2 . \tag{19}$$

One can see that these zones coincide with the limit of the instability zones (14) as $\gamma \to 0+$ for both simple and combination resonances. This is the special property of the external damping term $\gamma s(x) \partial w / \partial t$ used in (1). For other models of damping, the limit resonance zones for combination resonances are generally wider than those of the system with no damping (e.g. Seyranian and Mailybaev 2003).

If we fix the excitation amplitude $\delta$, the parametric resonance zone represents the half-ellipse in the $(\Omega, \gamma)$-plane, see Fig. 2(c). The size of this half-ellipse in the $\Omega$ and $\gamma$ directions is equal to $\Omega_{\rm res}(\delta, 0)$ and

$$\gamma_{\rm res}(\delta) = \sqrt{\frac{b_{ij}^2 (a_k^2 + b_k^2)}{4\omega_i \omega_j}} \, |\delta| \,, \tag{20}$$

respectively. The quantity $\gamma_{\rm res}(\delta)$ provides the maximal value of the damping coefficient, at which the parametric resonance is possible for a given excitation amplitude $\delta$.

## 4 Optimization problems

### 4.1 Maximization of the critical excitation amplitude

Let us fix the value of the damping coefficient $\gamma > 0$, and consider the shape of the beam maximizing the critical excitation amplitude $\delta_{\rm res}$ given by expression (17). Since the quantities $a_k$ and $b_k$ do not depend on $s(x)$, the optimal shape can be found by the minimization of the objective functional

$$\Phi(s) = \frac{|b_{ij}|}{\sqrt{\omega_i \omega_j}} = \frac{1}{\sqrt{\omega_i \omega_j}} \left| \int_0^1 u_i' u_j' \, {\rm d}x \right| \to \min \,. \tag{21}$$

The shape $s(x)$ appears in expression (21) implicitly through the eigenfrequencies $\omega_i$, $\omega_j$ and corresponding eigenmodes $u_i(x)$, $u_j(x)$, which are defined by (10) and boundary conditions (11). The critical excitation amplitude is expressed using the functional $\Phi$ as

$$\delta_{\rm res} = \frac{2\gamma}{\Phi \sqrt{a_k^2 + b_k^2}} \to \max \,. \tag{22}$$

The objective functional is decreased for larger eigenfrequencies $\omega_i$, $\omega_j$, and lower values of the integral containing slopes of the eigenmodes. Note that due to the integral in (21) the optimization problem is not equivalent to the maximization of the eigenfrequency $\omega_i$ in the case

of a simple resonance $i = j$. We will see below that, for the simply supported beam, the minimum of the objective functional $\Phi(s)$ is attained when both the eigenfrequency and the integral are decreased.

It is easy to see that the functional $\Phi(s)$ does not depend on the damping coefficient $\gamma$, on the resonance number $k$, or on the form of the excitation function $\varphi(t)$. Therefore, with the same optimal beam shape $s(x)$, the critical excitation amplitude is maximized for any damping coefficient, and in every resonance zone corresponding to a given mode ($i = j$) or a pair of modes ($i \neq j$). The optimal beam shape depends only on the modes involved in the resonance (indexes $i$ and $j$), on the static force $p_0$, and on the elastic coefficients in supports $c_1$ and $c_2$.

### 4.2 Minimization of the range of resonant excitation frequencies

Let us consider the width $\Delta\Omega_{\rm res}$ of the interval of resonant excitation frequencies for a specific resonance zone and fixed parameters $\gamma > 0$ and $\delta > \delta_{\rm res}(\gamma)$. This width is given by formula (18). We are going to find the shape $s(x)$ of the beam which minimizes $\Delta\Omega_{\rm res}$. Using the functional $\Phi$ defined in (21), we obtain

$$\Delta\Omega_{\rm res} = \frac{1}{k}\sqrt{(a_k^2 + b_k^2)\Phi^2\delta^2 - 4\gamma^2} \to \min\,. \tag{23}$$

Again, we arrive to the minimization problem (21). The shape of the beam, minimizing the range of resonant excitation frequencies $\Delta\Omega_{\rm res}$, is the same for any fixed damping coefficient $\gamma > 0$, excitation amplitude $\delta$, excitation function $\varphi(t)$, and resonance number $k$.

### 4.3 Universality of optimal designs

The analytical formulation of the optimization problem is to find the shape $s(x)$ minimizing the functional $\Phi(s)$ under the constant volume constraint (9). One can see that the optimal shape of the beam depends only on the modes involved in the resonance (indexes $i$ and $j$), on the constant compressive force $p_0$, and on the elastic support coefficients $c_1$ and $c_2$. This optimal shape has universal character, since it solves both the maximization problem for the critical excitation amplitude $\delta_{\rm res}(\gamma) \to \max$ with an arbitrary fixed damping coefficient $\gamma$ and the minimization problem for the resonant frequency range $\Delta\Omega_{\rm res}(\delta, \gamma) \to \min$ with arbitrary fixed $\delta$ and $\gamma$. Therefore, the half-cone resonance region (14) is minimized in both $\Omega$ and $\gamma$ directions. The optimal beam shape does not depend on the resonance number $k$ nor on the form of the periodic excitation function $\varphi(t)$. We note that these conclusions are based on the first-order approximation of the resonance zone (14) and, hence, they are valid under the assumption that $\delta$ and $\gamma$ are small.

## 5 Optimization method

### 5.1 Finite difference discretization

For numerical analysis of eigenfrequencies and eigenmodes, we reduce (10) to an algebraic eigenvalue problem using the finite difference method (e.g. Iwatsubo *et al.* 1973). For this purpose, we divide the interval $0 \le x \le 1$ into $n$ equal parts, see Fig. 3. At the middle of the $m$th part, $x_m = \frac{2m-1}{2n}$, we denote the values of the eigenmode $u(x)$ and the shape function $s(x)$ as

$$u_m = u(x_m)\,, \quad s_m = s(x_m)\,, \quad m = 1, \dots, n\,. \tag{24}$$

Then the finite difference approximation of (10) at $x_m$ takes the form

$$\left(\frac{s_{m-1}u''_{m-1} - 2s_m u''_m + s_{m+1}u''_{m+1}}{\Delta x^2}\right) + p_0 u''_m$$
$$= \omega^2 s_m u_m\,, \quad m = 1, \dots, n\,, \tag{25}$$

where

$$\Delta x = 1/n\,, \quad u''_m = \frac{u_{m-1} - 2u_m + u_{m+1}}{\Delta x^2}\,. \tag{26}$$

The values of $u_0$, $u_{-1}$ and $u_{n+1}$, $u_{n+2}$, required in the equations for $m = 1, 2, n-1$, and $n$, are found by using the finite difference approximation of boundary conditions (11) as

$$u_0 = -u_1\,, \quad u_{-1} = \frac{4c_1\Delta x}{s_1}\,u_1 - u_2\,,$$
$$u_{n+1} = -u_n\,, \quad u_{n+2} = -u_{n-1} + \frac{4c_2\Delta x}{s_n}\,u_n\,. \tag{27}$$

In the case of clamped left boundary condition, $c_1 = \infty$, we have $u_0 = u_1 = 0$ and the variable $u_{-1}$ is not needed. Analogously, in the case of clamped right boundary condition, $c_2 = \infty$, we have $u_n = u_{n+1} = 0$ and the variable $u_{n+2}$ is not needed.

Trapezoidal approximation is used for integral computations.

### 5.2 Discrete equations

As a result, (10) becomes the generalized symmetric eigenvalue problem of the form

$$\mathbf{Bu} = \omega^2\mathbf{Cu}\,, \tag{28}$$

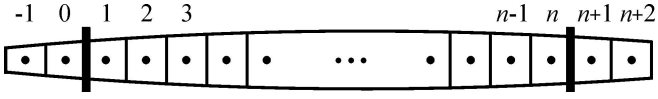


**Fig. 3** Beam divided into $n$ equal elements

where $\mathbf{u} = (u_1, \dots, u_n)^T$ is the eigenvector. The positive definite symmetric $n \times n$ matrix $\mathbf{B}$ is determined explicitly by (25)–(27). It depends on the discrete shape vector $\mathbf{s} = (s_1, \dots, s_n)^T$, static force $p_0$, and elastic coefficients of the supports $c_1$ and $c_2$. The $n \times n$ matrix $\mathbf{C} = \mathrm{diag}\,(\mathbf{s})$ is diagonal with the diagonal $\mathbf{s}$. Equation (28) determines $n$ eigenfrequencies $0 < \omega_1 < \ldots < \omega_n$ with the corresponding real eigenvectors $\mathbf{u}_1, \dots, \mathbf{u}_n$. The normalization condition (12) for the eigenvector $\mathbf{u}_i$ takes the form

$$\mathbf{u}_i^T \mathbf{C} \mathbf{u}_i = n\,, \tag{29}$$

where $\mathbf{u}_i^T$ denotes the vector transpose. In the case of clamped left (right) boundary condition, $c_1{=}\infty$ ($c_2{=}\infty$), the component $u_1$ ($u_n$) in the vector $\mathbf{u}$ is zero and can be omitted.

The constant volume constraint (9) becomes

$$\sum_{m=1}^{n} s_m = n\,, \tag{30}$$

and the objective functional (21) is approximated as

$$\Phi(\mathbf{s}) = \frac{\left|\mathbf{u}_i'^T \mathbf{u}_j'\right|}{n\sqrt{\omega_i \omega_j}} = \frac{\left|\mathbf{u}_i^T \mathbf{D}^T \mathbf{D} \mathbf{u}_j\right|}{n\sqrt{\omega_i \omega_j}}\,, \tag{31}$$

where the elements of the vector $\mathbf{u}_i' = (u_{i1}', u_{i2}', \dots, u_{in}')^T$ are found as

$$u_{im}' = \frac{u_{i(m+1)} - u_{i(m-1)}}{2\Delta x}\,, \quad m = 1, \dots, n\,. \tag{32}$$

Thus, $\mathbf{u}_i' = \mathbf{D}\mathbf{u}_i$, where nonzero elements of the $n \times n$ matrix $\mathbf{D} = [d_{ij}]$ are

$$d_{11} = d_{(m-1)m} = \frac{1}{2\Delta x}\,,$$
$$d_{m(m-1)} = d_{nn} = -\frac{1}{2\Delta x}\,, \quad m = 2, \dots, n\,. \tag{33}$$

In the case of simple resonances, $i = j$, expression (31) becomes

$$\Phi(\mathbf{s}) = \frac{\mathbf{u}_i^T \mathbf{D}^T \mathbf{D} \mathbf{u}_i}{n\omega_i}\,. \tag{34}$$

As additional constraints, we must consider $n$ inequalities

$$s_m \geq 0\,, \quad m = 1, \dots, n\,, \tag{35}$$

which are the natural conditions of non-negative beam width. The more general form of these constraints is

$$s_m \geq s_{\min}\,, \quad m = 1, \dots, n\,, \tag{36}$$

where $0 \leq s_{\min} < 1$ is the minimum allowed beam width.

## 5.3 Sensitivity analysis and optimization procedure

Derivatives of the eigenfrequency $\omega_i$ and eigenvector $\mathbf{u}_i$, satisfying (28) and normalization condition (29), with respect to components of the vector $\mathbf{s}$ can be found as (e.g. Seyranian and Mailybaev 2003)

$$\frac{\partial \omega_i}{\partial s_m} = \frac{1}{2n\omega_i}\, \mathbf{u}_i^T \left( \frac{\partial \mathbf{B}}{\partial s_m} - \omega_i^2 \frac{\partial \mathbf{C}}{\partial s_m} \right) \mathbf{u}_i\,,$$
$$\frac{\partial \mathbf{u}_i}{\partial s_m} = \mathbf{G}^{-1} \left( 2\omega_i \frac{\partial \omega_i}{\partial s_m} \mathbf{C} + \omega_i^2 \frac{\partial \mathbf{C}}{\partial s_m} - \right.$$
$$\left. \mathbf{u}_i \mathbf{u}_i^T \frac{\partial \mathbf{C}}{\partial s_m} - \frac{\partial \mathbf{B}}{\partial s_m} \right) \mathbf{u}_i\,, \quad m = 1, \dots, n\,, \tag{37}$$

where $\mathbf{G} = \mathbf{B} - \omega_i^2 \mathbf{C} + 2\mathbf{u}_i \mathbf{u}_i^T \mathbf{C}$ is a nonsingular matrix. With the use of expressions (37), derivatives of the objective function (31) are found in the form

$$\frac{\partial \Phi}{\partial s_m} = \frac{\mathrm{sign}\left(\mathbf{u}_i^T \mathbf{D}^T \mathbf{D} \mathbf{u}_j\right)}{n\sqrt{\omega_i \omega_j}} \times$$
$$\left( \frac{\partial \mathbf{u}_i^T}{\partial s_m} \mathbf{D}^T \mathbf{D} \mathbf{u}_j + \mathbf{u}_i^T \mathbf{D}^T \mathbf{D} \frac{\partial \mathbf{u}_j}{\partial s_m} \right) -$$
$$\left( \frac{\partial \omega_i}{\partial s_m} \omega_j + \omega_i \frac{\partial \omega_j}{\partial s_m} \right) \frac{\left|\mathbf{u}_i^T \mathbf{D}^T \mathbf{D} \mathbf{u}_j\right|}{2n(\omega_i \omega_j)^{3/2}}\,,$$
$$m = 1, \dots, n\,. \tag{38}$$

In the case of simple resonances, $i = j$, formula (38) becomes

$$\frac{\partial \Phi}{\partial s_m} = \frac{2}{n\omega_i}\, \mathbf{u}_i^T \mathbf{D}^T \mathbf{D} \frac{\partial \mathbf{u}_i}{\partial s_m} - \frac{\mathbf{u}_i^T \mathbf{D}^T \mathbf{D} \mathbf{u}_i}{n\omega_i^2} \frac{\partial \omega_i}{\partial s_m}\,. \tag{39}$$

Under a small variation of the beam shape $\mathbf{s} + \Delta\mathbf{s}$, the change of $\Phi$ can be approximated as

$$\Phi + \Delta\Phi = \Phi + \nabla\Phi \cdot \Delta\mathbf{s} + o\left(\|\Delta\mathbf{s}\|\right),$$
$$\nabla = \left( \frac{\partial}{\partial s_1}, \dots, \frac{\partial}{\partial s_n} \right). \tag{40}$$

The constant volume constraint (30) requires

$$\sum_{m=1}^{n} \Delta s_m = 0\,, \tag{41}$$

and the active width constraints (36) yield

$$\Delta s_m \geq 0 \quad \text{if} \quad s_m = s_{\min}\,, \quad m = 1, \dots, n\,. \tag{42}$$

Using expressions (40)–(42), the problem of minimizing the objective function $\Phi$ can be solved by using the gradient method. At each step, the function $\Phi$ and its derivatives are evaluated, and the redesign variation $\Delta\mathbf{s}$ is chosen in the steepest descent direction. This direction can be found as the projection of the vector $-\nabla\Phi$ onto the

subspace defined by (41) and active constraints (42). The necessary optimality conditions are

$$\frac{\partial \Phi}{\partial s_m} = \Psi_0 = const \quad \text{if} \quad s_m > s_{\min}\,,$$

$$\frac{\partial \Phi}{\partial s_m} \geq \Psi_0 \quad \text{if} \quad s_m = s_{\min}\,, \quad m = 1, \ldots, n\,. \tag{43}$$

These conditions were checked in the optimization process.

## 6 Optimal shapes of the beam

In this section, we analyse optimal shapes of the beam minimizing the size of simple resonance zones ($i = j$). These shapes depend on the mode number $i$, static compressive force $p_0$, and elastic support coefficients $c_1$ and $c_2$. In computations, we used $n = 100$ elements in the finite difference method. Comparing the results with the $n = 200$ elements approximation, we estimate the relative error of about 0.1% for the minimum value of objective function $\Phi$ and 0.2% for the shape function $s(x)$. As the initial shape, we consider the uniform beam with $s(x) \equiv 1$. For some cases, the global search with over than 1000 random nonsymmetric initial shapes was performed by using the $n = 20$ elements approximation. The computations showed that the obtained optimal designs correspond to the global minimum of the objective function.

### 6.1 Simply supported beam

A simply supported uniform beam ($c_1 = c_2 = 0$ and $s(x) \equiv 1$) has the dimensionless eigenfrequencies $\omega_i = \pi i \sqrt{\pi^2 i^2 - p_0}$, $i = 1, 2, \ldots$, where $p_0 < p_{\rm cr} = \pi^2$. For zero static compressive force, $p_0 = 0$, the optimal shape corresponding to the first mode ($i = 1$) is shown in Fig. 4 by a thin solid line. Here we did not use the minimum width constraint, i.e. we took $s_{\min} = 0$. The optimal beam has zero widths at the left and right supports. The values of the objective function for the uniform and optimal beams are equal to $\Phi_{\rm uniform} = 1$ and $\Phi_{\rm optimal} = 0.791$, respectively. Thus, the objective function describing the size of simple resonance zones corresponding to the first mode (see expressions (22) and (23)) is decreased by 20.9%.

The optimal shape corresponding to the second mode ($i = 2$) is shown in Fig. 4 by a thin dashed line. The optimal beam has zero widths at the supports and in the middle. Zero width in the middle of the beam can be physically treated as a hinge connecting two parts of the beam. But in this case, the deflection function $w(x, t)$ and the eigenmode $u(x)$ can have a discontinuity of the slope at $x = 0.5$. Such a beam becomes a mechanism losing stability at zero force. Therefore, the optimal shape of the beam corresponding to the second mode is physically irrelevant.

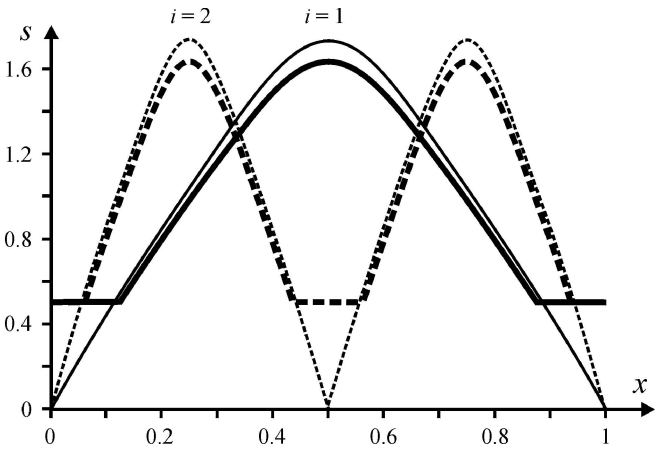


**Fig. 4** Optimal shapes of a simply supported beam

In order to avoid the situation when the width vanishes at some points, we can restrict the minimum beam width. By using constraints (36) with $s_{\min} = 0.5$, we find the optimal beam shapes for the first and second modes shown in Fig. 4 by bold solid and bold dashed lines, respectively. The relative reduction of the objective functional equals 17.67% and 17.74% for the first and second modes, respectively, which is about 3.2% less than for beam without the width constraint. The obtained solutions are physically correct and have practical form. We remark that the beam optimized with respect to the first mode has the static critical force $p_{\rm cr}^{\rm optimal1} = 11.49$, which is higher than the static critical force for the uniform beam $p_{\rm cr} = \pi^2 \approx 9.87$. But for the beam optimized with respect to the second mode, the static critical force $p_{\rm cr}^{\rm optimal2} = 7.97$ is lower than that of the uniform beam.

Dependence of the optimal shape on the static compressive force $p_0$ for the first mode is shown in Fig. 5, where the minimal width constraint $s_{\min} = 0.5$ is used. In this figure, $p_{\rm cr} = \pi^2$ denotes the critical force of the uniform beam. We notice that static critical forces of these optimal beams are higher than $\pi^2$. One can see that

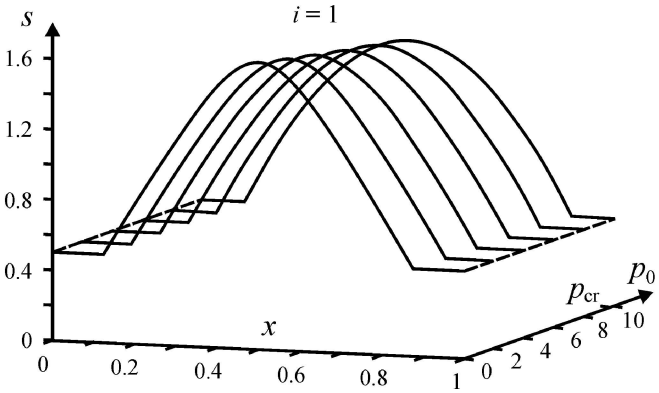


**Fig. 5** Optimal shapes of prestressed simply supported beams

the optimal shapes depend weakly on the compressive force $p_0$.

## 6.2 Clamped-clamped beam

The results for a clamped-clamped beam ($c_1 = c_2 = \infty$) and zero static compressive force ($p_0 = 0$) are presented in Fig. 6. The optimal shapes for the first and second modes ($i = 1$ and 2) are shown by solid and dashed lines, respectively. The thin and bold lines correspond to the unconstrained ($s_{\min} = 0$) and constrained ($s_{\min} = 0.5$) beam widths.

If the beam width is not restricted ($s_{\min} = 0$), the optimal beams have zero widths at internal points. Again, the optimal beam corresponding to the second mode is statically unstable at zero compressive force. In the case of the optimal beam corresponding to the first mode, the static loss of stability occurs when the central part is turned as a rigid body, and the right and left "ears" are buckled (see Seyranian and Privalova 2003). The corresponding static critical force is about 30% less than the critical force of the uniform beam. The relative decrease of the objective function $\Phi$ for the beam optimized with respect to the first mode is equal to 21.2%.

In the case of the restricted minimal width ($s_{\min} = 0.5$), we obtain practical optimal solutions, see Fig. 6 (bold lines). Compared to the uniform beam, the reduction of the objective functional is 18.63% and 18.80% for the optimal beams corresponding to the first and second modes, respectively. Computing optimal shapes of the beam for nonzero static compressive forces $p_0$ shows that these shapes are similar, with more material transferred from the middle to the areas near supports for bigger values of $p_0$.

After the width constraints being used, the static critical force of the beam optimized with respect to the first mode has been increased by about 4% compared to the uniform beam. Thus, the width constraint allows one to find clamped-clamped beams with higher resistance to parametric resonance without decrease in the static critical force. For the beam optimized with respect to the second mode, the static critical force is about 35% lower than that of the uniform beam. But this is still a big progress compared to zero critical force of the optimal beam without the width constraint.

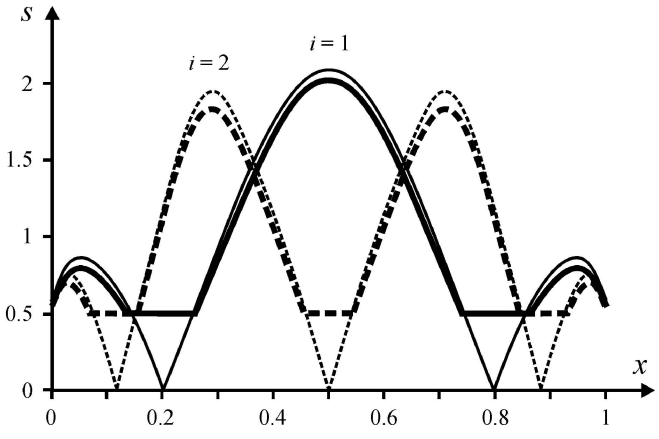


**Fig. 6** Optimal shapes of a clamped-clamped beam

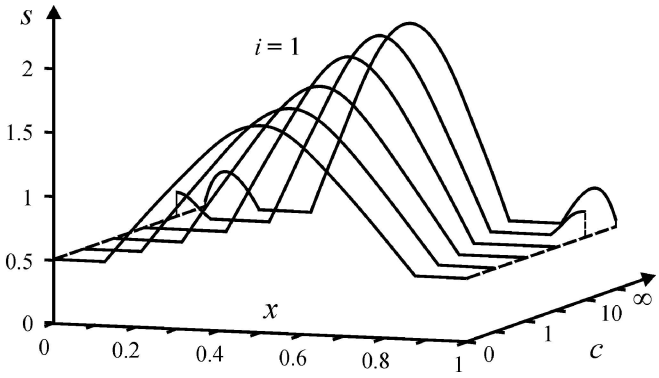


**Fig. 7** Optimal shapes of elastically supported beams for different elastic support coefficients $c$

## 6.3 Elastically supported beam

Finally, let us consider elastically supported beams with equal elastic coefficients of supports $c = c_1 = c_2$. Dependence of optimal beam shapes on the elastic coefficient $c$ is presented in Fig. 7, where the optimization was carried out for the first mode ($i = 1$), zero static compressive force $p_0 = 0$, and the width constraint $s_{\min} = 0.5$. Considerable dependence of the optimal shape on the elastic coefficient $c$ is observed. The relative decrease of the objective function for the optimal beam compared to the uniform beam varies between 17.7% and 20.4%, with the maximum at $c = 2.51$. With the increase of stiffness in the supports, more material of the optimal beam is concentrated in the middle part. For large stiffness coefficients $c$, additional material is required in the areas near the supports.

# 7 Experiment

In this section, we describe the experiment conducted for the uniform and optimal simply supported beams. The optimization is carried out for simple resonance zones of the first mode (lowest natural frequency) with zero static compressive force $p_0 = 0$ and the minimal width constraint $s_{\min} = 0.5$, which yields the optimal design shown in Fig. 4 by a bold solid line.

The test specimens are uniform and optimal beams manufactured by laser beam machining. The hinges are made of radial bearings (JIS 6200), which are accurately manufactured and have been cleaned by injecting a special oil with high pressure (Kure 556). One of the hinges is

rigidly clamped onto an aluminum slab. The other hinge is mounted on top of a sliding linear bearing (IKO Ball Slide Unit, Model BSU 44-50 A). On the lateral end of the linear bearing, a linear motor (Showa-Densen-Denran Model) delivers dynamic axial forces. A TOA Electronics waveform synthesizer model FS-2201 feeds the sinusoidal signal to a KIKUSUI power amplifier model BIPOLAR PBX40-10 which, in turn, drives the linear motor with required dynamic thrust force under current control. The deflection of the beam at the midpoint is measured by a laser sensor (KEYENCE model LB-60) which has a resolution of 40 $\mu$m and sampling time of 20 ms. The photograph of the experimental setting is shown in Fig. 8.

Phosphor-bronze beams are used in the experiments. The parameters of the uniform beam are:

$$m = 0.0322\,\mathrm{kg}\,, \quad l = 0.45\,\mathrm{m}\,, \quad h = 0.0008\,\mathrm{m}\,,$$
$$s_{\mathrm{uniform}} = 0.01\,\mathrm{m}\,, \quad \frac{h}{l^2}\sqrt{\frac{E}{12\rho}} = \frac{\omega_{\mathrm{uniform}}}{\pi^2} = 4.098\,\mathrm{s}^{-1}\,, \tag{44}$$

where $\omega_{\mathrm{uniform}}/(2\pi) = 6.437\,\mathrm{Hz}$ is the experimentally measured first natural frequency of the beam. The optimal beam has the same mass, length, and thickness. Recall that the value of the objective functional for the optimal beam is 17.67% less than for the uniform beam, $\Phi_{\mathrm{optimal}} = 0.8233$ and $\Phi_{\mathrm{unform}} = 1$.

Results of the experiment are given in dimensionless form (6) obtained with the use of quantities (44); the asterisks (*) are omitted. The dimensionless external damping coefficient $\gamma = 0.184$ is obtained by matching the theoretically computed decrement of free oscillations of the uniform beam with the experimental data.

Figure 9 shows the experimental response curves (amplitude of oscillations of the beam midpoint versus excitation frequency) for the uniform and optimal beams under the periodic force of fixed amplitude $\delta = 4.5$. There are two bifurcations: a subcritical bifurcation at the lower critical value of the excitation frequency $\Omega_{\mathrm{left}}$, and a supercritical bifurcation at the higher critical frequency

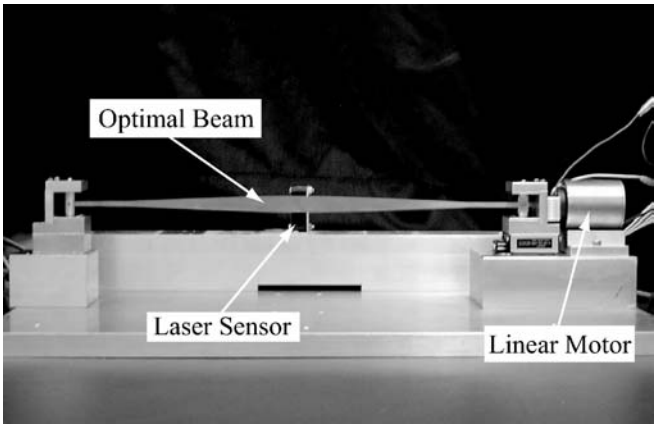


**Fig. 8** Experimental setup

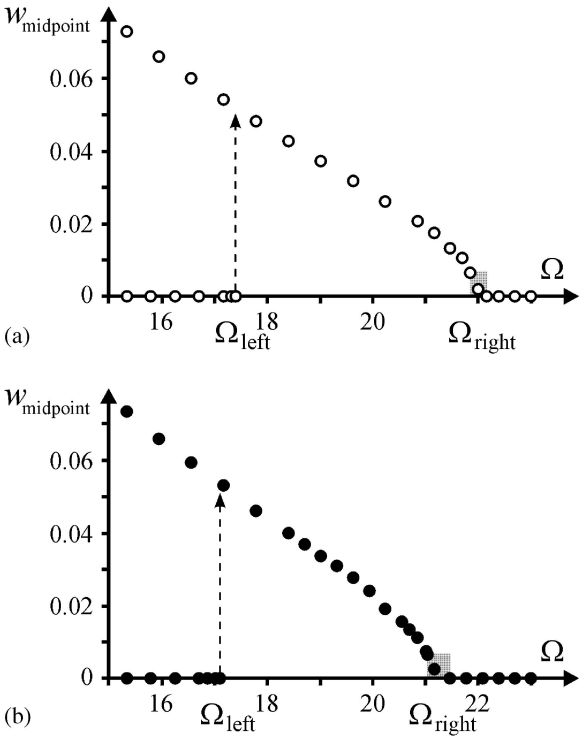


**Fig. 9** Experimental frequency response diagram for a fixed excitation amplitude: (a) uniform beam, (b) optimal beam

$\Omega_{\mathrm{right}}$. The small gray-shaded areas denote the frequency intervals where the beam motion is not regular periodic. This is caused by the Coulomb (static) friction at the supports, which becomes active due to a small amplitude of vibrations. The supercritical bifurcation is transcritical, which is caused by nonlinear quadratic damping (see Yabuno *et al.* 1998; Guckenheimer and Holmes 1983).

In order to regularize the measurements procedure, we used the following method. The left critical frequency $\Omega_{\mathrm{left}}$ is detected as a frequency at which the decay of the disturbance of size $w_{\mathrm{midpoint}} = 0.0033$ (1.5 mm) to the trivial state is changed by the jump to the nontrivial periodic motion. Notice that this finite disturbance is necessary to overcome static friction forces at the supports. The right critical frequency $\Omega_{\mathrm{right}}$ is detected as the frequency of regular periodic motion of the beam with the amplitude $w_{\mathrm{midpoint}} = 0.0067$ (3 mm). This value of the response amplitude corresponds roughly to the bound when the dynamics becomes influenced by static friction. The suggested measurements strategy gives the values of critical frequencies, which are slightly lower than the critical values for the system without static friction.

Figure 10 shows the boundaries of parametric resonance zones in the plane of frequency and amplitude of the excitation force. Empty and filled circles denote the experimental results for the uniform and optimal beams, respectively. Dashed and solid lines denote the corresponding theoretical results based on (14) and (21). One can observe a very good agreement of the experimental data with theoretical prediction. It is interesting to note that the resonant zone of the optimal beam is shifted to

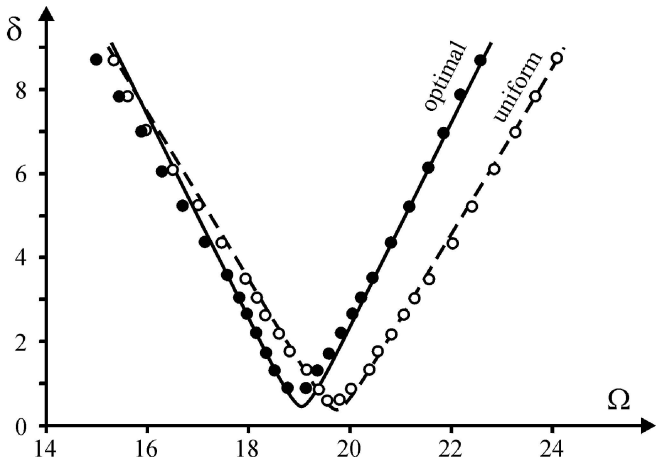


**Fig. 10** Boundary of the parametric resonance zone: uniform beam (○ experimental, – – – theoretical) and optimal beam (• experimental, —— theoretical)

the left, i.e. the natural frequency is decreased. Therefore, the minimum of the objective functional (21) is attained due to the big decrease of the integral containing the slope of the first natural mode of vibrations.

The experimental values for the ratio of resonant frequency intervals $\Delta\Omega_{\rm res}^{\rm optimal}/\Delta\Omega_{\rm res}^{\rm uniform}$ is shown in Fig. 11 by circles; solid line denotes the theoretical curve found by using formula (23). There is an excellent agreement between the experimental and theoretical data in the interval $3.5 \le \delta \le 8$. For lower amplitudes $\delta$, the reduction of the resonant frequency range is larger than predicted theoretically. But this difference can be well explained by the measurements errors, since the quantity $\Delta\Omega_{\rm res}^{\rm optimal}/\Delta\Omega_{\rm res}^{\rm uniform}$ represents the ratio of two small numbers for small values of $\delta$. For big values of the amplitude $\delta$, the reduction of the resonant frequency range is lower than predicted theoretically. This can be explained by the influence of second-order terms $\sim\delta^2$, which were neglected in the theoretical analysis, see Sect. 3.

Unfortunately, we cannot detect quantitatively the increase of the minimal (critical) resonant amplitude for the optimal beam. Since the damping is small in the system, the critical resonant amplitude appears to be in the region influenced by static friction. Nevertheless, in Fig. 10, one can see the qualitative increase of the critical resonant amplitude for the optimal beam relative to the uniform beam.

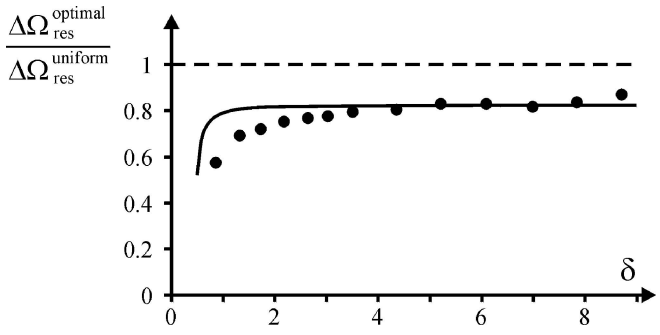


**Fig. 11** Reduction of the interval of resonant excitation frequencies for different values of the excitation amplitude $\delta$: • experimental and —— theoretical

Comparing the nonlinear behaviour of the uniform and optimal beams, see Fig. 9, we conclude that the beam's dynamics is described by the bifurcations of the same type: subcritical at $\Omega_{\rm left}$ and supercritical at $\Omega_{\rm right}$. Moreover, the optimal beam is "better" for its nonlinear characteristics, i.e. the amplitude of the nontrivial periodic motion for the optimal beam is smaller.

## 8 Conclusion

In this paper, we studied optimal shapes of elastic beams under the action of a periodic axial force. The excitation force amplitude and external damping coefficient are assumed to be small. Two optimization problems have been considered: the maximization of the minimal (critical) excitation amplitude and the minimization of the interval of resonant excitation frequencies for a fixed excitation force amplitude. It is shown that these two problems lead to the same objective function depending only on the frequencies and modes of free vibrations of the beam. Optimal beam shapes are found for different boundary conditions and resonant modes. The gain of the optimization is about 17–22% for the objective function depending on the boundary conditions and width constraints. The experiment conducted for simply supported uniform and optimal beams showed very good agreement with theoretical data.

From the practical point of view, the important feature of an optimal design is its weak sensitivity to a change of different parameters. We proved that the optimal beam shapes obtained in the paper do not depend on the amplitude and shape of the periodic force function, on the resonance number, nor on the external damping coefficient. Thus, the optimal beams possess strong universality property, and depend only on the boundary conditions and natural modes involved in the parametric resonance.

Only external damping was considered in this paper. As a topic for further investigation, it is interesting to study the influence of internal damping and damping in the supports on optimal shapes of the beam. This study can be carried out using the method suggested in this paper. We showed experimentally that the static friction is important for the analysis of nonlinear response of simply supported beams, which is another interesting subject. There are also mathematical issues to be studied. The parametric resonance zone can degenerate (a half-cone becomes a straight line) for higher order resonances, which requires higher order approximations for the stability analysis and optimization.

*Acknowledgements* This work was supported in part by the Japan Society for the Promotion of Science (JSPS) Fellowship

no. S-03217, and by the Russian Foundation of Basic Research grant no. 02-01-39004.

The first author is grateful to Alexander P. Seyranian, Yoshihiko Sugiyama, and Mikael Langthjem for useful suggestions and discussions on the topic of this paper, and to Hiroshi Yabuno and the students from his laboratory for the hospitality during the visit to the University of Tsukuba.

## References

Batchelor, G.K. 1999: *An introduction to fluid dynamics*. Cambridge: Cambridge University Press

Guckenheimer, J.; Holmes, P. 1983: *Nonlinear Oscillations, Dynamical Systems, and Bifurcations of Vector Fields*. New York: Springer

Iwatsubo, T.; Saigo, M.; Sugiyama, Y. 1973: Parametric instability of clamped-clamped and clamped-simply supported columns under periodic axial load. *J Sound Vib* **30**, 65–77

Langthjem, M.A. 1996: *Dynamics, stability and optimal design of structures with fluid interaction*, DCAMM Report no. S 71. Lyngby: Technical University of Denmark

Langthjem, M.A.; Sugiyama, Y. 2000: Dynamic stability of columns subjected to follower loads: a survey. *J Sound Vib* **238**, 809–851

Mailybaev, A.A.; Seyranian, A.P. 2001: Parametric resonance in systems with small dissipation. *J Appl Math Mech* **65**, 755–767

Pedersen, P. 1982–83: Design with several eigenvalue constraints by finite elements and linear programming. *J Struct Mech* **10**, 243–271

Seyranian, A.P.; Mailybaev, A.A. 2003: *Multiparameter Stability Theory with Mechanical Applications*. Singapore: World Scientific

Seyranian, A.P.; Privalova, O.G. 2003: The Lagrange problem on an optimal column: old and new results. *Struct Multidisc Optim* **25**, 393–410

Seyranian, A.P.; Solem, F.; Pedersen, P. 2000: Multiparameter linear periodic systems: sensitivity analysis and applications. *J Sound Vib* **229**, 89–111

Yabuno, H.; Ide, Y.; Aoshima, N. 1998: Nonlinear analysis of a parametrically excited cantilever beam (effect of the tip mass on stationary response). *JSME Int J Series C* **41**, 555–562